

---

Articles

---

2022-01-05

## Plasma induced reactive oxygen species-dependent cytotoxicity in glioblastoma 3D tumourspheres

Janith Wanigasekara

*Technological University Dublin, janith.manoharawanigasekara@tudublin.ie*

Carlos Barcia


*Universitat Autònoma de Barcelona*

Patrick J. Cullen

*University of Sydney*

*See next page for additional authors*

Follow this and additional works at: <https://arrow.tudublin.ie/creaart>

 Part of the [Biochemistry Commons](#), [Cancer Biology Commons](#), [Cell Biology Commons](#), [Molecular Biology Commons](#), and the [Oncology Commons](#)

---

### Recommended Citation

Wanigasekara, J., Barcia, C., Cullen, P. J., Tiwari, B., Curtin, J. F. Plasma induced reactive oxygen species-dependent cytotoxicity in glioblastoma 3D tumourspheres. *Plasma Processes Polym.* 2022; 19:e2100157. DOI: 10.1002/ppap.202100157

This Article is brought to you for free and open access by ARROW@TU Dublin. It has been accepted for inclusion in Articles by an authorized administrator of ARROW@TU Dublin. For more information, please contact [arrow.admin@tudublin.ie](mailto:arrow.admin@tudublin.ie), [aisling.coyne@tudublin.ie](mailto:aisling.coyne@tudublin.ie), [gerard.connolly@tudublin.ie](mailto:gerard.connolly@tudublin.ie).



This work is licensed under a [Creative Commons Attribution-NonCommercial-Share Alike 4.0 License](#)  
Funder: Science Foundation Ireland (SFI)

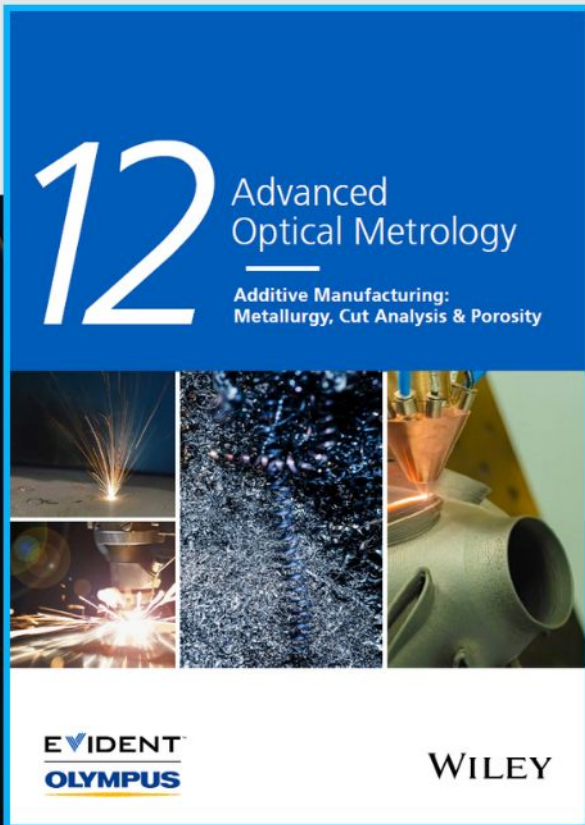
---

**Authors**

Janith Wanigasekara, Carlos Barcia, Patrick J. Cullen, Brijesh Tiwari, and James F. Curtin



# Additive Manufacturing: Metallurgy, Cut Analysis & Porosity



The latest eBook from  
**Advanced Optical Metrology.**  
Download for free.





In industry, sector after sector is moving away from conventional production methods to additive manufacturing, a technology that has been recommended for substantial research investment.

Download the latest eBook to read about the applications, trends, opportunities, and challenges around this process, and how it has been adapted to different industrial sectors.

**EVIDENT™**  
**OLYMPUS**

**WILEY**

# Plasma induced reactive oxygen species-dependent cytotoxicity in glioblastoma 3D tumourspheres

Janith Wanigasekara<sup>1,2,3,4</sup>  | Carlos Barcia<sup>5</sup> | Patrick J. Cullen<sup>1,6</sup>  |  
Brijesh Tiwari<sup>2</sup>  | James F. Curtin<sup>1,3,4</sup> 

<sup>1</sup>BioPlasma Research Group, School of Food Science and Environmental Health, Technological University Dublin, Dublin, Ireland

<sup>2</sup>Department of Food Biosciences, Teagasc Food Research Centre, Ashtown, Dublin, Ireland

<sup>3</sup>Environmental Sustainability & Health Institute (ESHI), Technological University Dublin, Dublin, Ireland

<sup>4</sup>FOCAS Research Institute, Technological University Dublin, Dublin, Ireland

<sup>5</sup>Institut de Neurociències, Department of Biochemistry and Molecular Biology, School of Medicine, Universitat Autònoma de Barcelona, Bellaterra, Spain

<sup>6</sup>School of Chemical and Biomolecular Engineering, University of Sydney, Sydney, Australia

## Correspondence

Janith Wanigasekara, BioPlasma Research Group, School of Food Science and Environmental Health, Technological University Dublin, Dublin, Ireland.  
Email: [janith.manoharawanigasekara@tudublin.ie](mailto:janith.manoharawanigasekara@tudublin.ie)

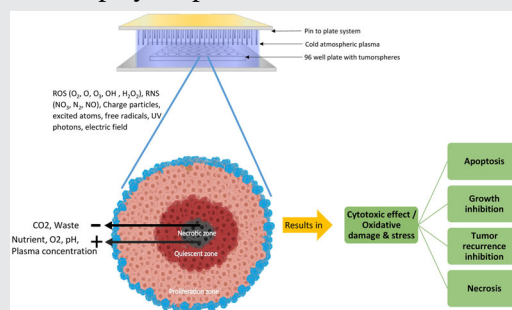
James F. Curtin, Dean of Engineering and Built Environment, Bioplasma Research Group, Technological University Dublin, Dublin, Ireland.  
Email: [james.curtin@tudublin.ie](mailto:james.curtin@tudublin.ie)

## Funding information

Science Foundation Ireland, Grant/Award Number: 17/CDA/4653; Teagasc Walsh Fellowships

## Abstract

The aim of this study was to determine the effects of a pin-to-plate cold atmospheric plasma (CAP) on U-251 MG three-dimensional (3D) glioblastoma spheroids under different conditions. 3D tumourspheres showed higher resistance to the CAP treatment compared to 2D monolayer cells. A single CAP treatment was able to induce cytotoxicity, while multiple CAP treatments augmented this effect. CAP was also able to induce cytotoxicity throughout the tumoursphere, and we identified that reactive oxygen species (ROS) plays a major role, while H<sub>2</sub>O<sub>2</sub> plays a partial role in CAP-induced cytotoxicity in tumourspheres. We conclude that ROS-dependent cytotoxicity is induced uniformly throughout glioblastoma and epidermoid tumourspheres by direct CAP treatment.



## KEYWORDS

3D tumourspheres, cold atmospheric plasma, cytotoxicity, epidermoid, glioblastoma, reactive oxygen and nitrogen species, ROS dependent

[Correction added on 12 January 2022, after first online publication: IReL funding statement has been added.]

This is an open access article under the terms of the Creative Commons Attribution License, which permits use, distribution and reproduction in any medium, provided the original work is properly cited.

© 2022 The Authors. *Plasma Processes and Polymers* published by Wiley-VCH GmbH



## 1 | INTRODUCTION

Glioblastoma multiforme (GBM) is a WHO grade IV astrocytoma, which is the most common and aggressive malignant primary brain tumor in adults. It has a low survival rate of less than 1 year for most patients and only about 5% survive beyond 5 years.<sup>[1–3]</sup> The existing standard therapy for GBM consists of surgical resection followed by radiation and chemotherapy.<sup>[3,4]</sup> However, the treatment and better outcomes for GBM are hampered by poor prognosis, high invasiveness, high resistance to chemotherapy, and the inability to traverse the blood-brain barrier.<sup>[1,3]</sup> Therefore, it is critical to identify novel technologies for efficacious *in vivo* glioblastoma diagnosis, prognosis, and treatment.

Plasma discharges can be classified as thermal or non-thermal plasma, with a further classification of cold atmospheric plasma (CAP) used to distinguish non-thermal plasmas, which are sufficiently low in temperature to allow their use in biological applications. CAP is a partially ionized gas that contains charged particles, reactive oxygen, and nitrogen species (RONS) (including hydroxyl, hydrogen peroxide, superoxide, hydroxyl radical, singlet oxygen, ozone, nitric oxide, nitrogen dioxide, dinitrogen tetroxide, nitrogen trioxide, nitrous oxide, and peroxyxynitrite), excited atoms, electrons, free radicals, UV photons, and electromagnetic fields.<sup>[5,6]</sup> Devices that generate CAP can be divided into: direct-discharge (i.e., dielectric barrier discharge (DBD), pin to plate system) and indirect-discharge (i.e., plasma jets, pens, and torches).<sup>[5,7]</sup> CAP-induced cancer cellular cytotoxicity has been demonstrated previously by using different devices, such as plasma jet,<sup>[8–12]</sup> micro-sized devices,<sup>[13]</sup> DBDs<sup>[14,15]</sup> and corona discharges. Previous studies have reported both direct and indirect CAP treatment efficacies in inducing anticancer effects (in numerous cancer types, such as pancreatic,<sup>[8]</sup> lung,<sup>[9,10]</sup> squamous cell carcinoma,<sup>[11]</sup> brain,<sup>[13]</sup> and so forth) in *in vitro*<sup>[8,9,11]</sup> and antitumor effects *in vivo*.<sup>[11–13]</sup>

Increasingly CAP is being explored as a novel therapeutic method for cancer treatment due to the fact that it operates at atmospheric pressure and near room temperature while having low power requirements.<sup>[16]</sup> Researchers have reported successful clinical applications of CAP to treat squamous cell carcinoma patients. Tumor reductions were reported by CAP treatment, along with increased tumor decontamination and reductions in tumor mass.<sup>[17]</sup> The trial demonstrates CAP's clinical utility in cancer treatment.

The chemical components such as reactive oxygen and nitrogen species (RONS) generated in plasma are found to induce biological effects, including structural damage to lipids in cell membranes, breakage of DNA, oxidization of proteins, initiation of different signaling pathways, and induced apoptosis.<sup>[5,6]</sup> Elevated levels of RONS are already produced in cancer cells compared to healthy cells and CAP

can further increase such RONS to cytotoxic levels. While our understanding of the biological and chemical effects of CAP on cancer cells is expanding, several gaps remain, for example, the effects of CAP on cells growing in a three-dimensional (3D) lattice. 3D cell culture models are beneficial for bridging the gap between *in vitro* cell cultures and *in vivo* responses by more closely mimicking the natural *in vivo* environment, shape, tissue stiffness, stresses, and cellular response while overcoming expenses and ethical considerations of animal models.<sup>[18–20]</sup> In comparison to 2D cell cultures, the addition of the third dimension in 3D cell culture affects the spatial organization of cell surface receptors that interact with other cells and imposes physical limits on cells. Spheroids' unique cyto-architecture simulates *in vivo* cellular topology, gene expression, metabolism, proliferation, oxygenation, nutrient uptake, waste excretion, and drug uptake while allowing cell–ECM connections and signaling to be maintained, hence regulating molecular processes and cellular phenotypes. ECM elements can also interact with cell surface receptors, including integrins and receptor tyrosine kinases. Integrin-growth factor receptor crosstalk controls downstream cell signaling and growth factor-induced biological activities, primarily proliferation and invasion. Furthermore, 3D tumorsphere cell–cell interactions are essential for juxtacrine signaling, where molecules travel directly between cells via gap junctions or other structures without being secreted into the extracellular environment. These receptor and juxtacrine signaling components modify a range of intracellular signaling pathways and in turn how cancer cells respond to their environment.<sup>[21,22]</sup>

However, due to higher aggressiveness and treatment resistance in GBM, there is a need to find an alternative to existing treatments by developing innovative approaches such as cold plasma technology.

In the present study, we used an *in vitro* 3D tumor spheroid model to better model the effects of CAP on glioblastoma cells.<sup>[23]</sup>

## 2 | MATERIALS AND METHODS

### 2.1 | Chemicals

All chemicals used in this study were supplied by Sigma-Aldrich—Merck Group unless stated otherwise.

### 2.2 | 2D cell culture

The human glioblastoma multiforme cell line (U-251 MG, formerly known as U-373MG-CD14) was a gift from Michael Carty (Trinity College Dublin) and the human epidermoid carcinoma (A431) were purchased from an ATCC European

Distributor (LGC Standards). The absence of mycoplasma was checked by using a MycoAlert PLUS Mycoplasma Detection kit (Lonza). Cells were maintained in Dulbecco's modified Eagle medium (DMEM)-high glucose supplemented with 10% fetal bovine serum (FBS) and 1% penicillin/streptomycin. Cells were maintained in a humidified incubator containing 5% CO<sub>2</sub> atmosphere at 37°C in a TC flask T25, standard for adherent cells (Sarstedt). Cells were routinely subcultured when 80% confluence was reached using 0.25% w/v Trypsin-EDTA solution.

### 2.3 | 3D cell culture

U-251 MG human glioblastoma multiforme (Figure 1c) and A431 human epidermoid carcinoma cells were used to generate tumor spheroids. Single-cell suspensions (with desired seeding density) were seeded into Nunclon™ Sphera™ 96-well-low attachment plates (Thermo Fisher Scientific) in

DMEM-high glucose supplemented with 10% FBS and 1% penicillin/streptomycin. The low attachment plates were centrifuged at 1250 rpm for 5 min for U-251 MG cells and 4000 rpm for 10 min for A431 cells followed by incubation (37°C, 5% CO<sub>2</sub>, 95% humidity).<sup>[24]</sup> Tumor spheroids formation was observed within 3 and 4 days for A431 and U-251 MG (Figure 1d), respectively. Tumor spheroid formation was visually confirmed daily using an Optika XDS-2 trinocular inverse microscope equipped with a Camera ISH500, and their mean diameters were analyzed using "ImageJ version 1.53.e" software. For growth analysis, varying numbers of U-251 MG cells (ranging from 2000 to 40 000 cells/ml) were seeded in the abovementioned Nunclon™ Sphera™ 96-well-low attachment plates for 14 days. Fresh media were added every third day by replenishing old media in each well without disturbing the tumorspheroids. The spheroid formation and growth were monitored daily by using an inverted phase-contrast microscope, and the sizes of the spheroids were measured as explained above for at least

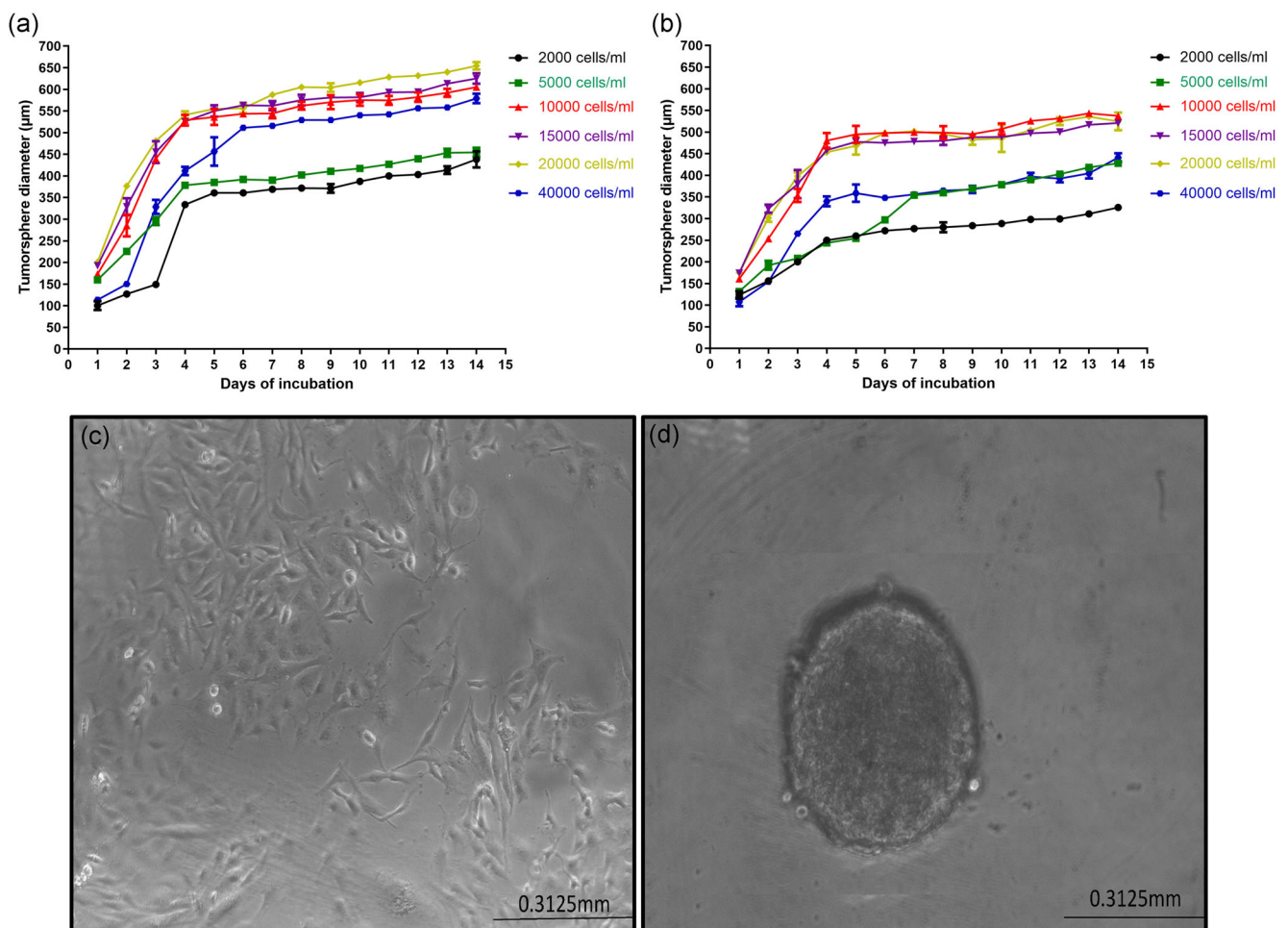


**FIGURE 1** Development of U-251 MG human glioblastoma astrocytoma 3D in vitro cell culture model. Growth kinetics analysis of U-251 MG spheroids at increasing seeding density in low attachment plate method (a) with serum medium. (b) Without serum medium. (c) Image of U-251 MG 2D cells in T75 flask taken using an optical microscope. (d) Image of U-251 MG 3D tumourspheres in low-adhesion Nunclon™ Sphera™ flat-bottom culture plate taken using an optical microscope

three independent experiments. Larger tumoursphere growth was observed when grown in DMEM high glucose media with 10% FBS compared to media without FBS. According to the initial seeding density, growth medium composition, and incubation time, the tumoursphere diameters varied from 100 to 650  $\mu\text{m}$ . The largest tumourspheres were observed with 10 000, 15 000, and 20 000 cells/ml initial seeding densities. It was also observed that exponential growth (Log) was achieved within the initial 4 days of growth, after which the growth curve became stationary, followed by a second growth phase after 7 days of incubation due to an increased number of dead cells inside the tumoursphere core (Figure 1). Two-way analysis of variance (ANOVA) demonstrated that there is a significant difference in tumoursphere (grown in serum medium) diameter between each initial seeding densities as shown in Figure 1a. However, there was no significant difference between diameters at Day 4, 5, and 6 in 10 000, 15 000, and 20 000 cells/ml seeding densities. In Figure 1b, there was no significant difference in tumoursphere (grown in without serum medium) diameter between the 10 000 and 20 000 cells/ml initial seeding densities. A full description of Tukey's multiple comparisons test is provided in the Supporting Information Sections (D1 and D2).

## 2.4 | Pin to plate system

A pin to plate electrode design was employed to generate a large volume atmospheric discharge. The reactor consisted of 88 slightly convex pins attached to stainless steel electrode (150  $\times$  200 mm), paired with a flat stainless steel ground plate (200  $\times$  250 mm) powered by an AC power supply (Leap100, PlasmaLeap Technologies). The schematic and image of the pin-to-plate device demonstrating the position of the microplates for cell treatment is shown in Figure S1. This Leap100 power supply has a discharge voltage up to 80 kV (p-p), resonance frequency from 30 to 125 kHz, discharge frequency from 100 to 3000 Hz, and power from 50 to 700 W. The air gap between the pin electrodes and the ground plate serves as the sample treatment area, with all samples in this study being placed in the center. All the samples were treated at a resonant frequency of 55.51 kHz, with a discharge frequency of 1000 Hz and duty cycle of 73  $\mu\text{s}$ , while the discharge gap was kept at 40 mm. The pin to plate system configurations, electrical characterization, and optical diagnostics were previously detailed by Scally et al.<sup>[25]</sup> Cells were treated for a time range of 0–320 s. The electrodes/sample treatment area was covered in a fitted container to minimize escape of CAP-generated reactive species into the general environment.

## 2.5 | Cell viability assay

Cell viability was analyzed using Alamar Blue™ cell viability reagent (Thermo Fisher Scientific). U-251 MG and A431 cells were seeded at a density of  $1 \times 10^4$  cells/well (100  $\mu\text{l}$  culture medium/well) into flat-bottom 96-well plates (Sarstedt, Ltd.) and were seeded at a density of  $1 \times 10^4$  cells/well (200  $\mu\text{l}$  culture medium/well) into Nunclon™ Sphera™ 96-Well -low attachment plates (Thermo Fisher Scientific), respectively, for 2D and 3D cell culture. Cells were incubated overnight at 37°C in a humidified atmosphere. DMEM media without sodium pyruvate supplemented with 10% FBS and 1% penicillin/streptomycin, DMEM media supplemented with 0.11 g/L sodium pyruvate with 10% FBS, and 1% penicillin/streptomycin and DMEM media supplemented with 0.11 g/L sodium pyruvate with 1% penicillin/streptomycin and without 10% FBS were used in this study as indicated.

In the 2D cell culture, after 24 h incubation, 70%–80% confluence was checked, 75  $\mu\text{l}$  of media was removed, leaving 25  $\mu\text{l}$  of media for treatment in each well. In the tumoursphere culture, after 3 days of incubation for A431 and 4 days incubation for U-251 MG, 175  $\mu\text{l}$  of media was removed, leaving 25  $\mu\text{l}$  of media for treatment in each well, unless otherwise specified. Cells/tumourspheres were then treated with direct plasma exposure at six different time points (0, 20, 50, 100, 160, and 320 s) using a discharge voltage of 46 kV, frequency of 1000 Hz, and using a duty cycle of 73  $\mu\text{s}$ . 75  $\mu\text{l}$  (for 2D) and 175  $\mu\text{l}$  (for 3D) of fresh culture media was added immediately following CAP treatment and incubated at 37°C using 5% CO<sub>2</sub> for 24, 48, 72, and 96 h. Dimethyl sulfoxide (DMSO) (20%) was used as a positive control. Single or multiple CAP treatments were carried out for the tumourspheres, where multiple treatments are a combination of three individual treatments with a 24 h incubation gap between each treatment.

After the post treatment incubation, tumourspheres were washed with sterile phosphate-buffered saline (PBS), trypsinized using 0.25% w/v trypsin–EDTA solution, and incubated for 3 h at 37°C with a 10% Alamar Blue™ solution. Fluorescence was measured using an excitation wavelength of 530 nm and an emission wavelength of 590 nm with a Varioskan Lux multi-plate reader (Thermo Scientific). All experiments consisted of at least three independent tests with a minimum of 30 replicates per experiment.

## 2.6 | Live/dead cell staining using propidium iodide (PI)

After CAP treatment the well media was immediately replenished with the plates incubated at 37°C with 5% CO<sub>2</sub> for 24, 48, 72, and 96 h. For PI staining, the media was removed

and the tumourspheres were washed with PBS and trypsinized using 0.25% w/v trypsin–EDTA solution into a single-cell suspension. Then trypsin was inactivated and cells were collected from each treatment point into a single centrifuge tube for centrifugation at 250g for 5 min. The supernatant was then aspirated, and the pellet re-suspended in 1 ml of 1× PBS. PI was then added to the cell suspension at 10 µg/ml and incubated for 1 min in the dark. PI fluorescence was then measured using the Beckman Coulter CytoFLEX Flow Cytometer with a blue laser (488 nm).

## 2.7 | PI staining and confocal imaging

Tumourspheres were seeded in a Nunclon Sphera 60 mm dish (Thermo Fisher Scientific) at a density of  $1 \times 10^5$  cells/ml and incubated at 37°C using 5% CO<sub>2</sub> for 4 days. After tumoursphere formation, the media was removed, following 320 s of CAP treatment, and fresh media was added to the dish and incubated at 37°C using 5% CO<sub>2</sub> for 24 h. After incubation, tumourspheres were rinsed three times with PBS and incubated with pre-warmed (37°C) Propidium Iodide (10 µg/ml) containing media for 10 min at 37°C. Cells were then washed once with PBS and loaded into fresh PBS. Tumourspheres were transferred to 35 mm glass-bottom dishes (Greiner Bio-One) and observed using a Zeiss LSM 510 confocal laser scanning microscope.

## 2.8 | 3D rendering

Representative confocal Z-scans of tumorspheres were processed for 3D reconstructions and visualization of the cell death penetration after treatment. Contrasted dichroic stacks of images were rendered with 3D iso-surfaces in computerized software (Surface tool, Imaris Bitplane) to limit the external border of the spheres. Then, PI-positive nuclei were detected by positive fluorescence voxels as individual spots (Spots tool, Imaris Bitplane) considering the adequate threshold and resolution. Then, PI-positive spots were labeled with an undefined color code according to the 3D distance to the border. 3D rotations of the tumorspheres and the addition of clipping planes were performed in rendering software to show the representative stack of images.

## 2.9 | ROS scavenger assays

Reactive oxygen species (ROS) inhibitor N-acetyl cysteine (NAC) was used as a ROS scavenger. Tumourspheres were seeded and constructed as previously described. For

the dose-response curves, tumourspheres were incubated for 3 h at 37°C with 4 mM NAC in DMEM in the presence and absence of pyruvate. 175 µl of media was removed and the tumourspheres were exposed to CAP. Post treatment, fresh media containing 4 mM of NAC was added and the cells were incubated at 37°C using 5% CO<sub>2</sub> for 24, 48, 72, and 96 h. The same procedure was carried out for the multiple CAP-treated samples. Cell viability was measured using the Alamar Blue™ assay. NAC titration was performed by exposing the tumourspheres to a range of 0–8 mM NAC with cell viability assessed after 96 h.

## 2.10 | Detecting ROS production using H2DCFDA assay

A cell permeant nonfluorescent probe, 2,7-dichlorodihydrofluorescein diacetate (H2DCFDA) (Thermo Fisher Scientific), was used to measure ROS generated by CAP treatment. H2DCFDA is a chemically reduced form of fluorescein converted to the highly fluorescent 2',7'-dichlorofluorescein (DCF) after the cleavage of the acetate groups by intracellular esterases and oxidation. U-251 MG tumourspheres were seeded in a Nunclon Sphera 60 mm dish (Thermo Fisher Scientific) at a density of  $1 \times 10^5$  cells/ml using DMEM high glucose in the absence of sodium pyruvate and incubated at 37°C using 5% CO<sub>2</sub> for 4 days. Subsequently, the culture medium was removed and the tumourspheres were washed with 1× PBS. Tumourspheres were incubated with replenished DMEM media, without sodium pyruvate and phenol red, containing 25 µM H2DCFDA for 1 h at 37°C. Tumourspheres were washed with fresh medium once and then with 1× PBS and then exposed to CAP at different time points (20, 160, and 320 s). Following CAP treatment, tumourspheres were incubated for 3 h at 37°C using 5% CO<sub>2</sub>. Tumourspheres were trypsinized into a single cell suspension and all liquids, including media, washing PBS, and trypsinized cell suspension were collected and centrifuged at 1200 rpm for 5 min. Cells were re-suspended in 1× PBS with fluorescence measured using a Beckman Coulter CytoFLEX Flow Cytometer with a 488 nm blue laser for excitation and FL1 standard filter for H2DCFDA measurement.

## 2.11 | Hydrogen peroxide scavenger assay

Catalase (E.C. 1.11.1.6) is an antioxidant enzyme that is found in peroxisomes, it catalyzes the decomposition of H<sub>2</sub>O<sub>2</sub> to form water and molecular oxygen ( $2 \text{H}_2\text{O}_2 \rightarrow 2 \text{H}_2\text{O} + \text{O}_2$ ).<sup>[26]</sup> U-251 MG tumourspheres were seeded in



Nunclon™ Sphera™ 96-well-low attachment plates (Thermo Fisher Scientific) at a density of  $1 \times 10^5$  cells/ml and incubated at 37°C using 5% CO<sub>2</sub> for 4 days. Catalase stock solution (1 mg/ml equivalent to 2000–5000 units/ml) was freshly prepared in 1× PBS, and diluted in fresh media to 0.1 mg/ml for inhibition of H<sub>2</sub>O<sub>2</sub> production. After the formation of the tumourspheres, replenished DMEM media, without sodium pyruvate and phenol red, containing 0.1 mg/ml catalase were incubated for 1 h at 37°C. CAP treatment was performed on the samples for 160 and 320 s. Then the fresh media with catalase was added to the dish and incubated at 37°C using 5% CO<sub>2</sub> for 24 h. After incubation, PI staining was carried out as explained in Section 2.6. PI fluorescence was then measured using a Beckman Coulter CytoFLEX Flow Cytometer with a blue laser (488 nm).

## 2.12 | Statistical analysis

All the experiments were replicated at least three independent times. Prism versions 9.1.0, GraphPad Softwares, Inc. were used to carry out curve fitting and statistical analysis. Dose-response curves were measured using nonlinear regression. Data are presented as a percentage and error bars of all figures were presented using the standard error of the mean (SEM), multiple comparison analyzes were performed using Tukey's test unless otherwise stated. CytExpert software was used for flow cytometry analysis and the mean of FITC-A was used to plot the reading results in columns statistics. PI uptake studies were analyzed using two-way ANOVA with Tukey's post-test.

## 3 | RESULTS AND DISCUSSION

### 3.1 | Pin-to-plate discharge presents cytotoxicity toward GBM cells in a time/dose-dependent manner

The tumor microenvironment plays a key role in tumor progression, metastasis, angiogenesis, cytotoxicity resistance, and immune cell modulation.<sup>[27,28]</sup> We employed a U-251 MG 3D cell culture model, which enabled cell–cell and cell–ECM interactions in all three dimensions and mimicked diffusion-limited distribution of oxygen, nutrients, metabolites, and signaling molecules common in the microenvironment of in vivo tumors. Most of the research on the effects of CAP on cancer cells has been investigated by using 2D monolayer cell cultures<sup>[29,30]</sup> and a growing number of animal models.<sup>[11,13]</sup> There are also a few studies carried out using the pin to plate design<sup>[25,29]</sup>; however, this is the first

time that we are reporting the approach for induced cytotoxicity in 3D tumor spheroids.

We have tested tumorsphere growth with different seeding densities and observed tumoursphere growth ranging from 100 to 650 μm in diameter. Our findings correlate with the tumourspheres sizes obtained by Singh et al.<sup>[31]</sup> We used this diffusion-limited 3D cell culture model to explore the diffusion of cytotoxic reactive species throughout the tumoursphere, rate of cell death, and effects of single and multiple CAP treatments on the cell–cell and cell–ECM interactions.

The tumoursphere size and resistance to CAP treatment were enhanced when tumourspheres were cultured in media containing serum, which is in agreement with others.<sup>[32]</sup> Previous studies from our research group demonstrated that the optimal discharge frequency using the pin to plate reactor was 1000 Hz, producing the highest overall RONS within the plasma. Correspondingly, the highest cytotoxic responses were also observed for 1000 Hz.<sup>[25]</sup> We, therefore, used a resonant frequency of 55.51 kHz with a discharge frequency of 1000 Hz and a duty cycle of 73 μs for exploring the technology's potential for 3D cell cultures.

First, the effects of plasma discharge on the GBM tumourspheres were studied under two different media compositions (DMEM high glucose with and without the presence of 10% FBS). Plasma-treated tumourspheres were post incubated at 24, 48, and 96 h at 37°C. An IC<sub>50</sub> of 386.3 s ( $375.9 \pm 397.1$  s), 460.7 s ( $449.4 \pm 472.4$  s), and 769.3 s ( $742.5 \pm 797.0$ ) were found for tumourspheres grown in a media with serum, CAP-treated, and post incubated at 24, 48, and 96 h, respectively. An IC<sub>50</sub> of 82 s ( $80.68 \pm 83.33$  s), 172.4 s ( $170.3 \pm 174.6$  s), and 237.4 s ( $230.5 \pm 244.5$  s) were found for tumourspheres grown in media without serum, CAP-treated, and post incubated at 24, 48, and 96 h, respectively (Figure 2a). Two-way ANOVA demonstrated that there is a significant difference in viability between the doses of CAP, different post treatment incubations, and media used for tumoursphere growth ( $p < 0.0001$ ). A full description of Tukey's multiple comparisons test is provided in the Supporting Information Section D3. According to these results, tumourspheres grown in high glucose DMEM with 10% FBS showed higher CAP resistance (Figure 2a) and growth rate (Figure 1a), likely more similarly reflecting the in vivo conditions. Hence, we use media supplemented with 10% serum for all further tumourspheres to get a better representation of the in vivo effects.

Next, we compare the effects of the plasma discharge on U-251 MG human glioblastoma multiforme and A431 human epidermoid carcinoma (2D and 3D cells) in DMEM high glucose with 10% FBS medium after 24 h incubation time. An IC<sub>50</sub> of 386.3 s ( $375.9 \pm 397.1$  s) and 160.4 s ( $157.0 \pm 163.9$  s) were found for U-251 MG 3D and 2D cells, respectively and an IC<sub>50</sub> of 125.5 s ( $123.2 \pm 127.9$  s) and

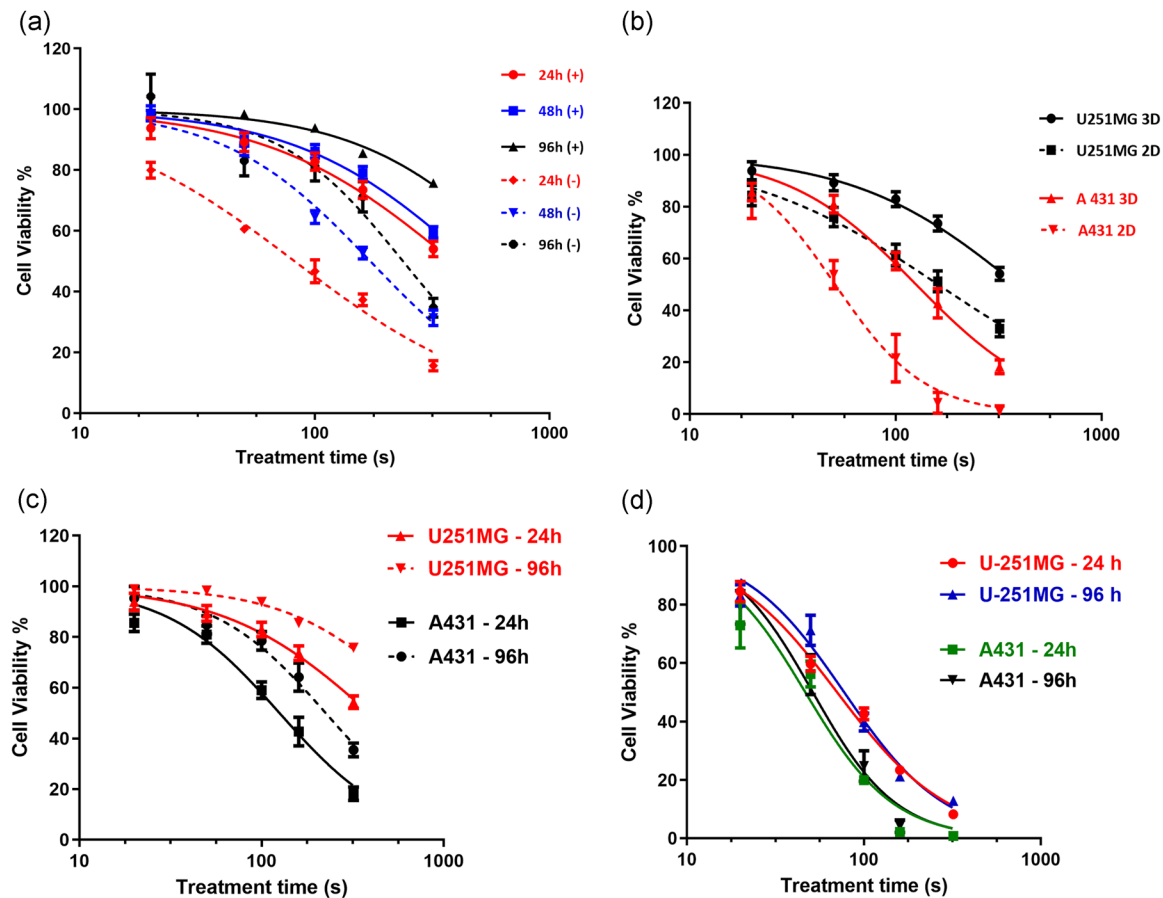


**FIGURE 2** U-251 MG cold atmospheric plasma (CAP) treatment. (a) U-251 MG tumoursphere single CAP treatment and post treatment incubation at 24, 48, and 96 h [with serum media represented as a (+) and without serum media represented as (-)]. (b) U-251 MG and A431 3D, 2D cell cytotoxicity comparison after CAP treatment and 24 h post treatment incubation. (c) Comparison of U-251 MG and A431 single CAP treatments with 24 and 96 h incubations. (d) Comparison of U-251 MG and A431 multiple CAP treatment with 24 and 96 h incubation

50.77 s ( $49.67 \pm 51.90$  s) were found for A431 3D and 2D cells, respectively (Figure 2b). Two-way ANOVA shows that there is a significant difference in U-251 MG and A431 (2D and 3D) cell viability between the doses of CAP and different cell lines ( $p < 0.0001$ ). A full description of Tukey's multiple comparisons test can be seen in the Supporting Information Section D4. When using a single CAP treatment, U-251 MG 3D tumoursphere displayed greater resistance to CAP compared with the 2D cell cultures with U-251 MG cells also showing a higher treatment resistance compared to the A431 cell lines.

Subsequently, we determine the cytotoxic effects of a single CAP treatment on GBM tumourspheres (in DMEM media with and without sodium pyruvate). These data confirmed that the pyruvate-free media resulted in greater effects. Depending on the cytotoxicity results (Figure S2), the single plasma discharge did not induce full cytotoxicity in the tumourspheres, even at the highest dose at 24 h incubation (320 s, cell viability = 49.16%–58.94% in Figure S2b).

Since the single CAP treatment was not enough to induce higher cytotoxicity and halt tumor regrowth, we hypothesized that the use of multiple (three consecutive daily) CAP treatments would result in more favorable outcomes. The two-way ANOVA demonstrated that there is a significant difference in viability between each dose of multiple CAP, different post treatment incubations, and media used for tumoursphere growth ( $p < 0.0001$ ). A full description of Tukey's multiple comparisons test can be seen in the Supporting Information Section D5 (Figure S2a) and D6 (Figure S2b). The differences in  $IC_{50}$  values and significant difference between different media used (DMEM high glucose with and without pyruvate) shows a protective effect of sodium pyruvate. These experiments identified multiple CAP treatments as the most successful way to induce effective cytotoxicity in the target tumourspheres.

To compare plasma effectivity toward different cell lines, single and multiple CAP treatments of both U-251 MG and A431 tumourspheres were carried out. For single CAP treatment, cell viability after 24 h was 54.33% ( $IC_{50}$ –390.6 s)

and 18.22% ( $IC_{50}$ –125.5 s) for U-251 MG and A431 tumourspheres, respectively, with the highest dose (320 s) (Figure 2c). CAP-treated tumourspheres incubated for a longer time period (96 h) led to cell viability increases in both cell lines. Cell viability with the highest dose was found to be 75.83% ( $IC_{50}$ –777.3) and 35.46% ( $IC_{50}$ –225.0) for U-251 MG and A431 tumourspheres, respectively (Figure 2c).

The kinetic response to CAP treatment over time was markedly different. For 2D cultures, significantly more cell death was evident 96 h after treatment compared with 24 h, with cytotoxicity found to be ROS-dependent.<sup>[29]</sup> Conversely, for both U-251 MG and A431 3D tumourspheres, the

induced cytotoxicity after 24 h was proportional to the plasma dosage but was found to partially recover their RONS damage and regrow, similar to previous reports<sup>[14]</sup> and in contrast to cells grown in the 2D monolayer.<sup>[29]</sup> Our data also shows that the U-251 MG cell line is highly resistant to single-dose plasma treatments and is able to regrow quickly when compared to A431. These results have important implications for future animal model and human trials where single CAP treatments may be insufficient to yield significant benefits.

For the multiple CAP treatments and incubation at 24 h, cell viability with the highest dose was 8.22%

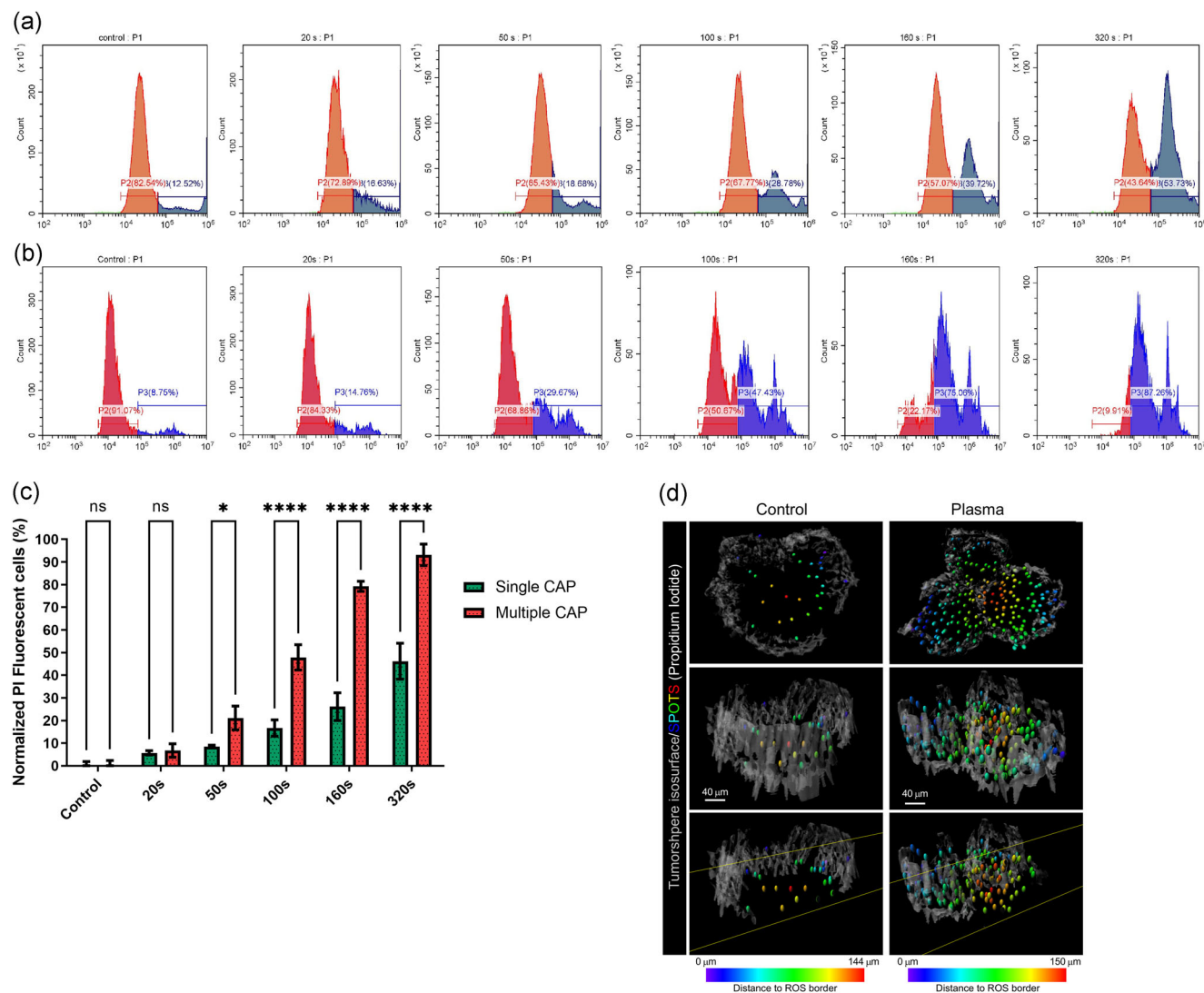


**FIGURE 3** PI uptake in pin-to-plate-treated U-251 MG tumourspheres. PI uptake was measured by flow cytometry and used as an indicator of cell death. Cells were treated at 240 V, 1000 Hz, and 73  $\mu$ s for 0, 20, 50, 100, 160, and 320 s. PI uptake was then measured 24 h post treatment in (a) single cold atmospheric plasma (CAP) treatment, (b) multiple CAP treatments, (c) normalized PI uptake was then measured at 24 h post single and multiple treatments and represented as a bar chart. All the data points were statistically significant except control and 20 s treatment times. (d) Fluorescence levels of control and 320 s CAP treated, PI stained U-251 MG tumourspheres observed by confocal microscopy detected by 3D software. Tumoursphere cell death identified in each spot and distance to reactive oxygen species (ROS) border shown. Distance to the ROS border is color-coded according to the scale at the bottom. ns, not significant, \* $p \leq 0.05$ ; \*\*\*\* $p \leq 0.0001$

(IC<sub>50</sub>-70.59) and 0.76% (IC<sub>50</sub>-46.65) for U-251 MG and A431 tumourspheres, respectively (Figure 2d). With a post treatment incubation of 96 h, cell viability was 12.82% (IC<sub>50</sub>-77.38) and 0.59% (IC<sub>50</sub>-51.44) for U-251 MG and A431 tumourspheres, respectively (Figure 2d). The results confirmed that U-251 MG human glioblastoma multiforme tumourspheres were more resistant to plasma treatment when compared to the A431 human epidermoid carcinoma. However, multiple CAP treatments significantly induced cytotoxicity in tumourspheres and it was able to fully/partially inverse tumoursphere regrowth ability in A431/U-251 MG, respectively. Multiple CAP doses successfully reduced U-251 MG tumoursphere regrowth rates.

Two-way ANOVA demonstrated that there is a significant difference in the viability between single and multiple CAP doses, post treatment incubation period, and cell line used for tumoursphere growth ( $p < 0.0001$ ). A full

description of Tukey's multiple comparisons test is available in the Supporting Information Section D7 (Figure 2c) and D8 (Figure 2d). Based on the analysis it is demonstrated that the pin to plate device could induce tumoursphere cytotoxicity in a dose- and time-dependent manner.

### 3.2 | Effect of CAP treatment on tumoursphere cell membrane damage

PI was used to validate the pin-to-plate- induced cell death and cytotoxicity in U-251 MG tumourspheres. PI is a membrane-impermeable, fluorescent, nucleic acid intercalating agent, allowing identification of dead cells with compromised plasma membranes in a population in tumourspheres. PI uptake was measured 24 h post single (Figure 3a) and multiple

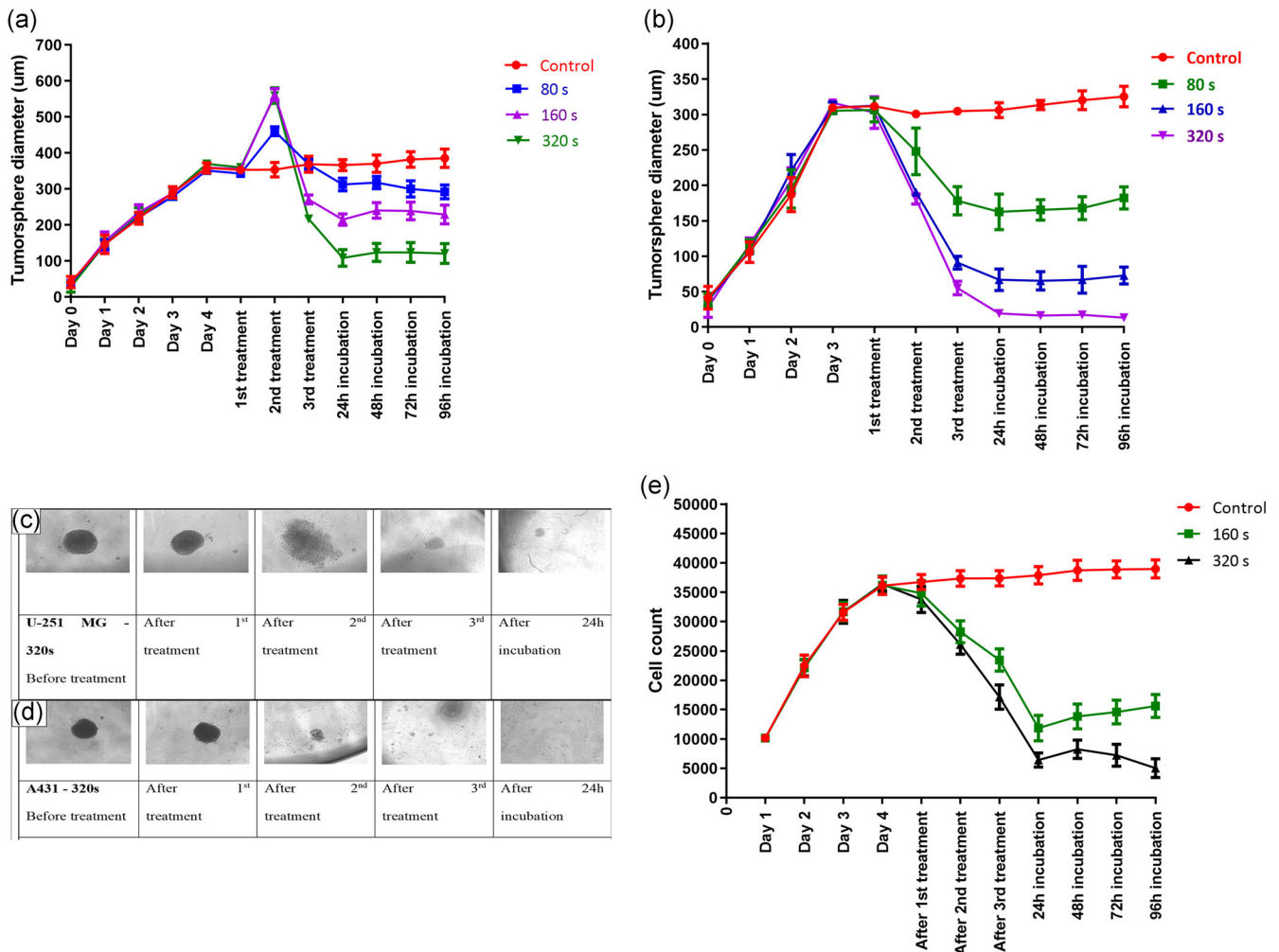


**FIGURE 4** U-251 MG and A431 tumoursphere size (diameter) and cell count analysis followed by cold atmospheric plasma (CAP) treatment. (a) U-251 MG, (b) A431, (c) U-251 MG tumoursphere morphological changes with CAP treatment. (d) A431 tumoursphere morphological changes with CAP treatment (converted all of the panels [c] and [d] to grayscale and applied a simple linear brightness adjustment [+40%]). (e) U-251 MG tumoursphere cell count change with multiple CAP treatment



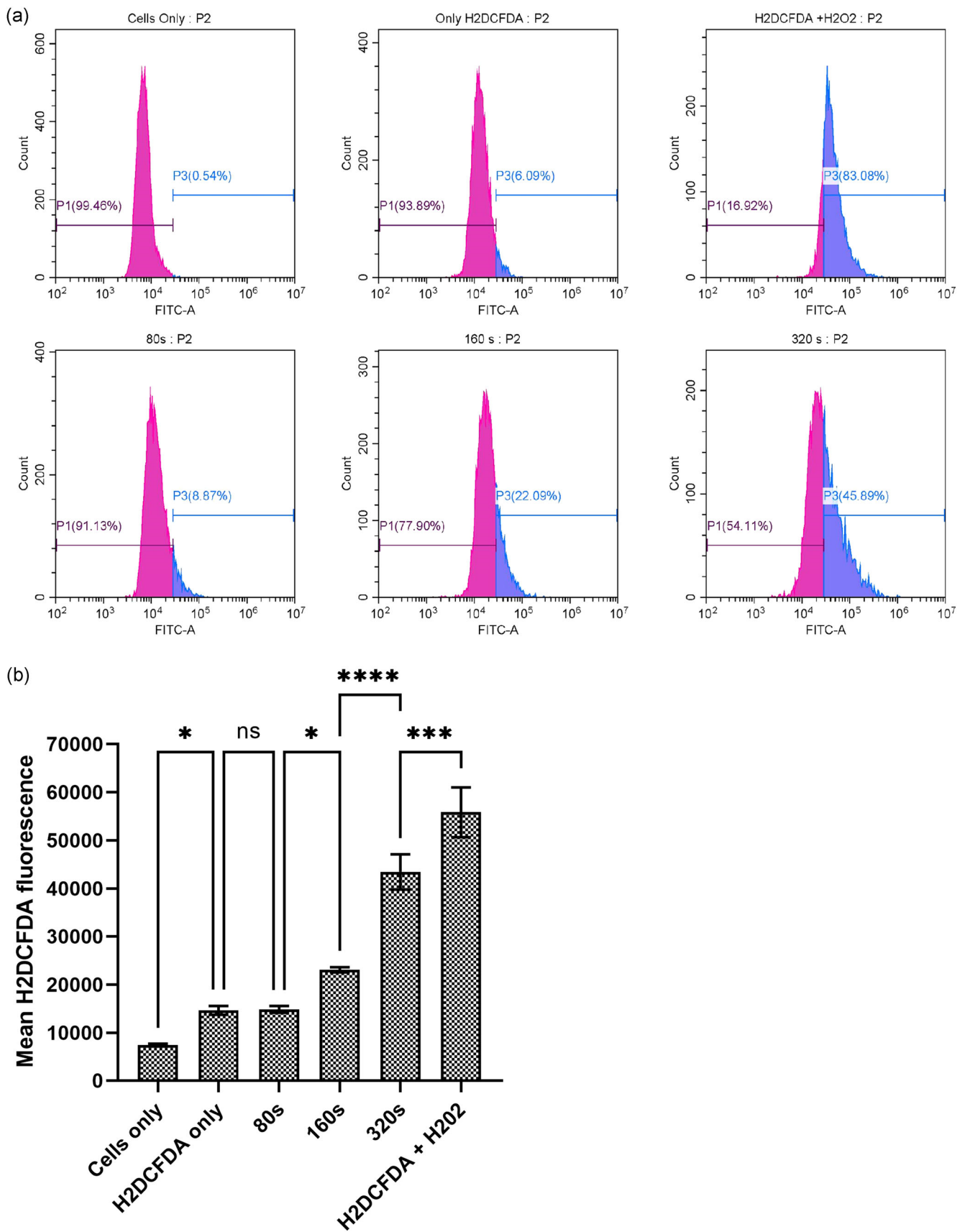


FIGURE 5 (See caption on next page)

(Figure 3b) CAP treatments. The PI uptake increased to almost 45% and 90%, respectively, following single and multiple CAP treatments for 320 s as shown in Figure 3c. This also proves that CAP treatment can damage the tumoursphere's cell membrane and induce cytotoxicity. This validates the Alamar blue™ assay data.

Two-way ANOVA demonstrated that there was a significant difference in PI uptake between control and the 50, 100, 160, and 320 s doses ( $p < 0.0001$ ), while no significant difference was found between the control and 20 s for both single and multiple CAP treatment. A full description of Tukey's multiple comparisons test can be seen in the Supporting Information Section D9.

The outer layer of the spheroid is exposed to the surrounding medium and is mainly composed of viable, proliferating cells.<sup>[33]</sup> It is tempting to hypothesize that when tumourspheres are exposed to CAP, gas-phase reactive species are first trapped by the surrounding medium and then initiate chemical reactions on the outer layer of cells, this then leads to cell death in the outer layer of cells, resulting in weakened cell–cell interactions and the disassembly of the tumoursphere. It was reported that despite the ability of RONS to penetrate throughout the entire depth of 3D tumourspheroids, apoptosis was observed only on the outermost layer or surface.<sup>[9]</sup> However, this is not what occurs in our case. We used confocal microscopy alongside a 3D reconstruction of stacked images to build three-dimensional maps of the treated tumourspheres. The distance of each dead cell to the nearest surface of the tumoursphere was calculated and color-coded (Figure 3d). With this analysis, we demonstrated that cytotoxicity, measured by PI uptake, increased significantly after multiple treatments. Even after a single CAP treatment, we observed a uniform distribution of dead cells throughout the tumoursphere. These data underscore the capacity of ROS generated by CAP to diffuse at least 150  $\mu\text{m}$  from the surface of the tumor without limiting cytotoxicity, and that low doses of CAP (single treatments) cause a significant disruption of cell–cell and cell–ECM interactions throughout the tumoursphere.

### 3.3 | CAP induced morphological changes

Changes in the tumoursphere morphology induced by CAP treatment were studied to get a better understanding of their mechanism of cell death. Tumoursphere diameter was found to be significantly reduced after the third CAP treatment (320 s) for both U-251 MG (Figure 4a) and A431 (Figure 4b) cell lines. Representative tumoursphere images showing the morphological changes induced by 320 s CAP treatment for U-251 MG and A431 are shown in Figures 4c and 4d, respectively.

Multiple CAP treatments induced significant, cumulative cytotoxicity. This was manifested by spheroid shrinkage and markedly reduced tumor regrowth ability, which was achieved with lower overall doses of CAP. It is therefore likely that multiple CAP treatments over a relatively short period of time would be necessary for clinical applications, setting constraints on approaches to deliver CAP directly to the tumor site. Interestingly, the response of U-251 MG and A431 tumourspheres to multiple CAP treatments was visibly different. Whereas U-251 MG tumourspheres (Figure 4a) had no appreciable morphological change after the first treatment, swelled significantly at the second treatment, and broke apart after the third treatment; A431 tumourspheres (Figure 4b) reduced in size after the first treatment and gradually broke apart on consecutive treatments. Overall, the outcome was essentially the same with enhanced cytotoxicity and inability to reform tumourspheres after multiple treatments, but the effects suggest that the cell–cell and cell–ECM interactions are different for each cell line.

Finally, to validate the above changes after multiple CAP treatments, we calculated the number of cells in the tumoursphere (cells/ml) accompanied by 0, 160, and 320 s CAP treatments. The number of cells in a tumoursphere rapidly declined during each CAP treatment with the lowest cell number observed after a 24 h post treatment incubation period. Subsequently, the number of cells increased slightly for the 160 s treatment with the overall cell amount slowly decreasing with the 320 s treatment (Figure 4e). Interestingly, U-251 MG tumoursphere diameter increased during the second CAP treatment (Figure 4a) while reducing cell number

**FIGURE 5** Reactive oxygen species production in U-251 MG tumourspheres. 3D cells were incubated with H2DCFDA and treated at three different doses of cold atmospheric plasma (a) 3 h post treatment cells were collected and analyzed using CytExpert software. (b) The mean of the FITC channel was used to plot the values on columns and analyzed using one-way ANOVA with Tukey's post-test (Supporting Information Section D11). All the data points were statistically significant except H2DCFDA only and 80 s treatment times. ns, not significant ( $p > 0.05$ ); \* $p \leq 0.05$ ; \*\*\* $p \leq 0.001$ ; \*\*\*\* $p \leq 0.0001$

(Figure 4e). It is possible that multiple CAP treatments can weaken cell–cell and cell–ECM interactions, and due to this, the volume of the densely arranged tumorsphere started to increase, resulting in an increased tumorsphere diameter. On the other hand, a higher number of cells were dead and detached from the tumorsphere core, which was observed as a reduction in cell number. Two-way ANOVA demonstrated that there was a significant difference in the number of cells during the 24–96 h incubation period ( $p < 0.0001$ ). A full description of Tukey's multiple comparison test is available in the Supporting Information Section D10.

### 3.4 | ROS production in U-251 MG tumourspheres

We evaluated intracellular reactive oxygen species by using H2DCFDA, a cell-permeable probe. Analysis of the histograms show significantly increasing levels of intracellular-oxidized H2DCFDA and ROS as a function of treatment time (Figure 5a). The mean fluorescence levels of 80, 160, and 320 s CAP-treated tumourspheres were increased by a factor of 1, 1.6, and 3 times, respectively, compared to the negative control (Figure 5b).

### 3.5 | Pin-to-plate presents RONS-dependent cytotoxicity

Tumoursphere response observed in the presence and absence of sodium pyruvate from single and multiple

CAP treatments may indicate the presence of ROS-dependent cytotoxic effects. The ROS-induced cytotoxic effect of the pin to plate system was evaluated by using different treatment time points (0, 20, 50, 100, 160, and 320 s) with *N*-acetyl-L-cysteine (NAC) employed as a ROS scavenger.

The highest CAP treatment resistance was evident in the tumourspheres treated in the high glucose DMEM with pyruvate and NAC. The second highest cytotoxicity resistance was observed in the high glucose DMEM without pyruvate and with NAC. The highest cytotoxicity was shown in tumourspheres treated in high glucose DMEM without pyruvate or NAC and high glucose DMEM with pyruvate and without NAC, respectively (Figure 6). This confirms that the cytotoxicity induced by the pin system is mainly dependent on RONS. NAC significantly protected the target tumourspheres from CAP-induced cytotoxicity at each applied dose, post treatment incubation period, media compositions, and single/multiple treatments ( $p < 0.0001$ ), whereas sodium pyruvate did not significantly protect against cytotoxicity. A full description of Tukey's multiple comparisons test and all the  $IC_{50}$  values and ranges are shown in the Supporting Information Section (Table S1 and D12–D17).

Titration of NAC was performed to confirm the optimum working concentrations. Two-way ANOVA demonstrated that there was no significant difference between 2, 4, and 8 mM of NAC, showing that increases or decreases in NAC concentration of around 2–8 mM do not change the protective effects (Figure S3 and D18 in Supporting Information Section).

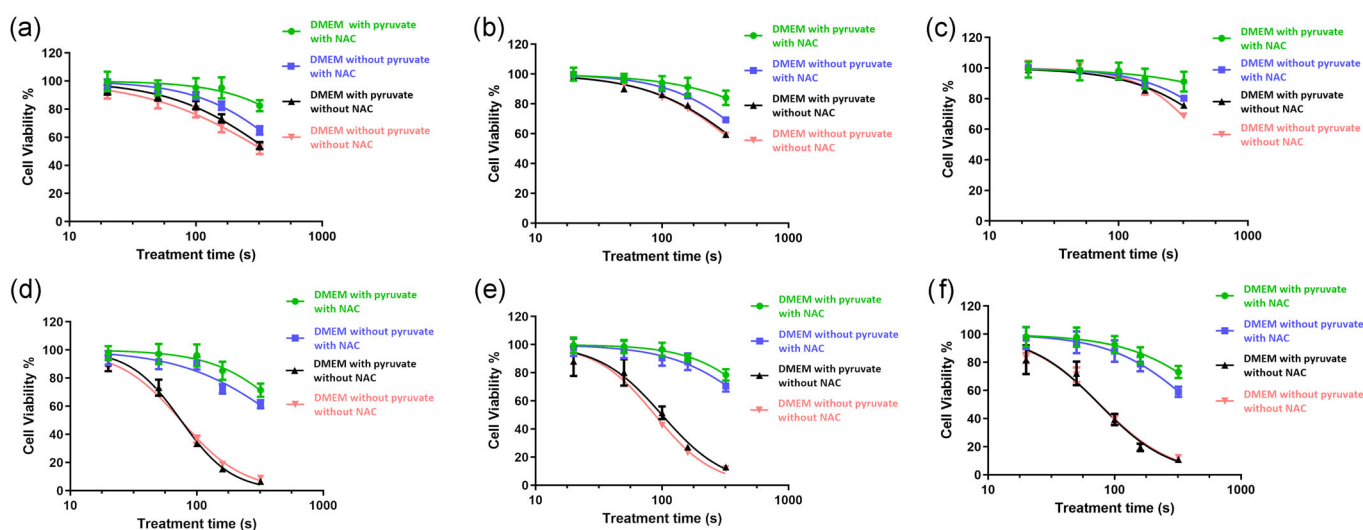


FIGURE 6 U-251 MG single and multiple cold atmospheric plasma (CAP) treatment with and without *N*-acetyl cysteine in with and without pyruvate media. (a) Single CAP 24 h, (b) single CAP 48 h, (c) single CAP 96 h, (d) multiple CAP 24 h, (e) multiple CAP 48 h, (f) multiple CAP 96 h incubation

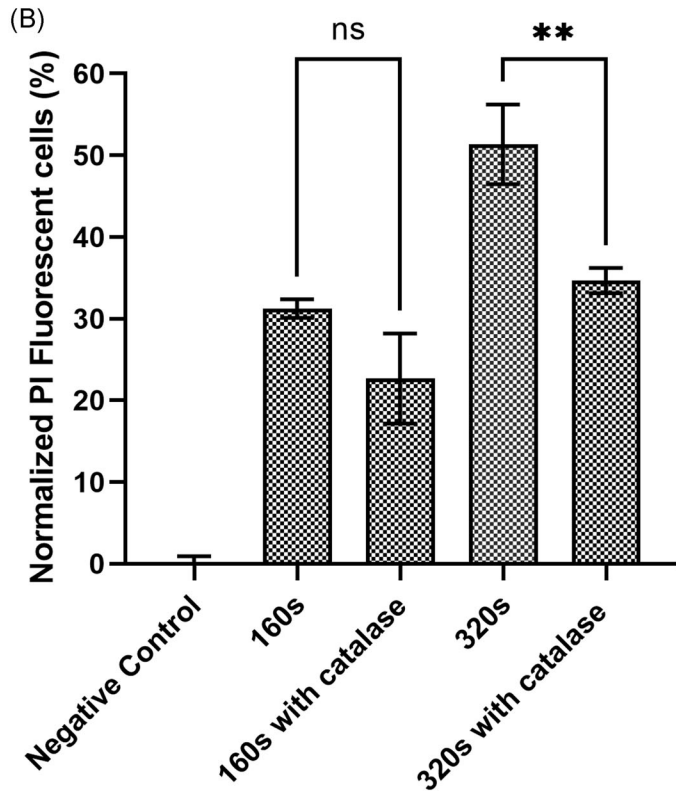
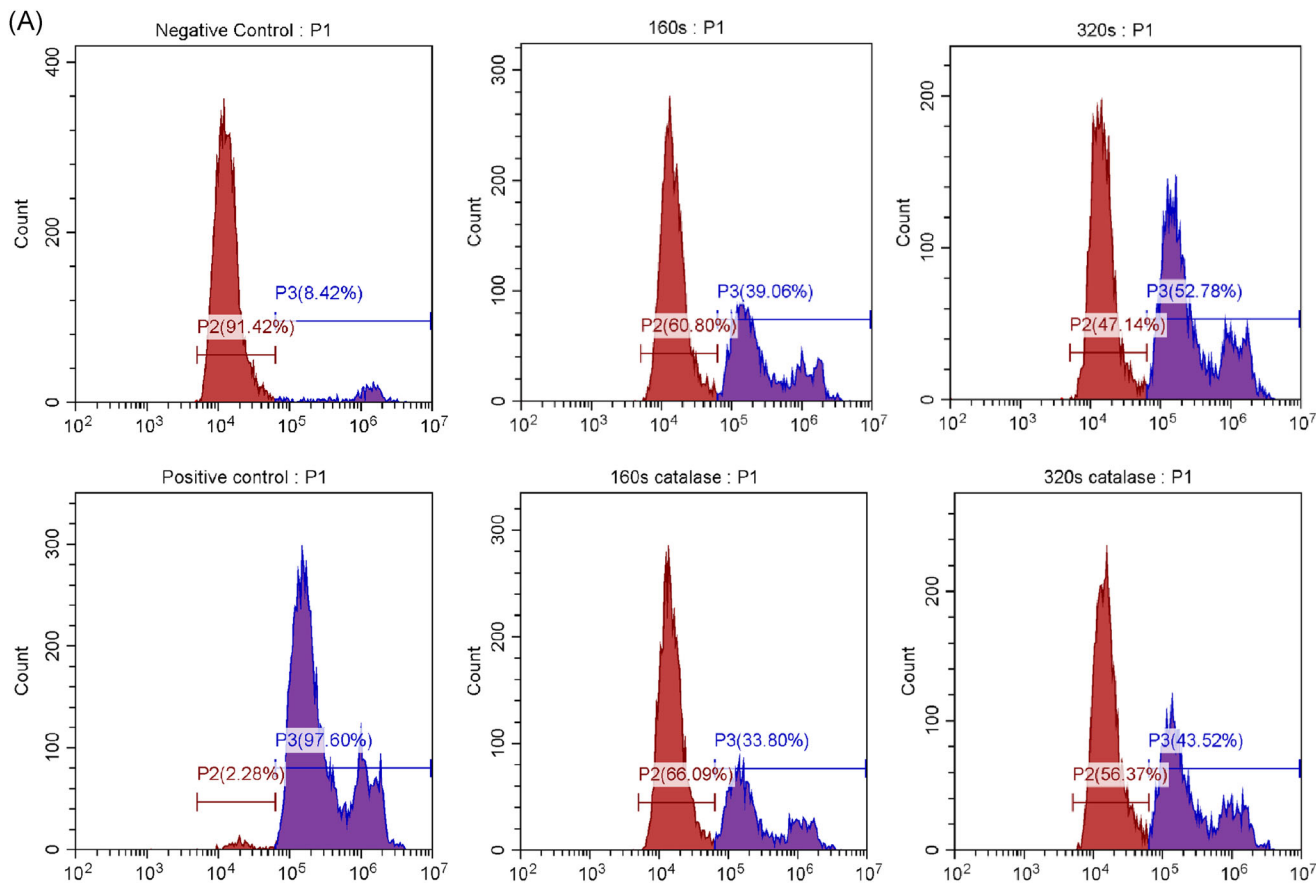


FIGURE 7 (See caption on next page)



### 3.6 | Catalase as hydrogen peroxide scavenger

PI uptake was measured 24 h after a single CAP treatment (160, 320 s) and compared to PI uptake with and without catalase (Figure 7a). Catalase reduced the PI uptake slightly from 31% to 23% after 160 s CAP treatment, while it significantly reduced cytotoxicity from 51% to 34% after 320 s CAP treatment (Figure 7b). There was no significant difference between 160 s with and without catalase, while there was a significant difference between 320 s with and without catalase. According to this experiment, catalase is able to slightly reverse the CAP-induced cytotoxicity, proving that hydrogen peroxide generated in pin to plate device contributes to the observed tumoursphere cytotoxicity.

Plasma-induced apoptosis in tumoursphere was previously shown to depend on  $\text{H}_2\text{O}_2$ ,  $\text{NO}_2^-$ , and  $\text{NO}_3^-$  and it is demonstrated that these diffuse longer distances than short-lived species, such as  $\text{O}_2^-$ ,  $\text{OH}\cdot$ , and  $\text{ONOOH}/\text{ONOO}^-$ .<sup>[28,30]</sup> In our case, cell-permeable NAC is protective, yet catalase was unable to fully protect cells from CAP, indicating that reactive species other than hydrogen peroxide also play a role in the 3D tumoursphere model. Therefore, the response of U-251 MG tumourspheres to CAP is different from previous reports, and indeed to U-251 MG cells grown in 2D cultures where we found, using the same plasma system where CAP treatment induced predominantly  $\text{H}_2\text{O}_2$ -dependent cytotoxicity.<sup>[29]</sup> Together, our data indicate a relative resistance of U-251 MG tumourspheres to hydrogen peroxide during CAP-induced cell death. Cell death may instead be mediated by other ROS species we have previously measured in the plasma plume or media, including  $\text{OH}$ ,  $\text{N}_2$  second positive system,  $\text{N}_2^+$  first negative system, nitrate, and ozone.<sup>[25]</sup> Alternatively, direct generation of intracellular ROS may account for some of the cytotoxicity observed.

## 4 | CONCLUSION

CAP treatment can effectively induce 3D glioblastoma tumoursphere cell death in a time-, dose-, treatment-frequency, and ROS-dependent manner. CAP is also able

to reduce 3D glioblastoma spheroid growth and cell proliferation and induce damage to the tumor micro-environment. CAP generated from the pin to plate device induces cytotoxicity throughout the tumoursphere, likely via long-lived RONS ( $\text{H}_2\text{O}_2$ ,  $\text{NO}_2^-$ , and  $\text{NO}_3^-$ ) and also other reactive species, with multiple treatments augmenting this cytotoxic effect. Our results indicate the importance of CAP-generated long and short-lived species for the growth inhibition and cell cytotoxicity of solid glioblastoma tumors, as they are necessary to achieve a sustained reduction of 3D glioblastoma spheroids in vitro. Furthermore, our results set important limitations on the likely approach needed when translating CAP into a clinical setting, with an approach that allows multiple treatments favorable over a single treatment.

### ACKNOWLEDGMENTS

This study was supported by Science Foundation Ireland (SFI) under Grant Number 17/CDA/4653 and funded through Teagasc Walsh Fellowship. The authors also thank TU Dublin, ESHI, and FOCAS Research Institutes for the use of facilities and support of technical staff. Open access funding enabled and organized by IREL.

### CONFLICT OF INTERESTS

Author Patrick J. Cullen, a CEO of PlasmaLeap Technologies. PlasmaLeap Technologies supplied the Leap100 power supply and pin-to-plate reactor used in this study.

### DATA AVAILABILITY STATEMENT

The data that support the findings of this study are available from the corresponding author upon reasonable request.

### ORCID

Janith Wanigasekara  <https://orcid.org/0000-0003-0962-3434>

Patrick J. Cullen  <http://orcid.org/0000-0001-7654-6171>

Brijesh Tiwari  <https://orcid.org/0000-0002-4834-6831>

James F. Curtin  <http://orcid.org/0000-0002-9320-9254>

### REFERENCES

- [1] S. Lapointe, A. Perry, N. A. Butowski, *Lancet (London, England)* **2018**, 392(10145), 432.
- [2] J. Bi, S. Chowdhry, S. Wu, W. Zhang, K. Masui, P. S. Mischel, *Nat. Rev. Cancer* **2020**, 20(1), 57.

**FIGURE 7** PI uptake in cold atmospheric plasma (CAP) treated U-251 MG tumourspheres in the presence and absence of catalase. PI uptake was measured by flow cytometry and used as an indicator of cell death. PI uptake was measured 24 h post treatment. (a) Histograms of negative control, 160 s CAP treated with and without catalase, 320 s CAP treated with and without catalase and positive control. (b) Normalized PI uptake was then measured at 24 h post treatment, represented as a bar chart and analyzed using one-way ANOVA with Tukey's post-test (Supporting Information Section D19). ns, not significant ( $p > 0.05$ );  $**p \leq 0.01$

- [3] A. Mariappan, G. Goranci-Buzhala, L. Ricci-Vitiani, R. Pallini, J. Gopalakrishnan, *Cell Death Differ* **2021**, *28*(1), 15.
- [4] B. S. Mahmoud, A. H. AlAmri, C. McConville, *Cancers* **2020**, *12*(1), 175.
- [5] D. Braný, D. Dvorská, E. Halašová, H. Škovierová, *Int J Mol Sci* **2020**, *21*(8), 2932.
- [6] X. Dai, K. Bazaka, E. W. Thompson, K. K. Ostrikov, *Cancers* **2020**, *12*(11), 3360.
- [7] A. Malyavko, D. Yan, Q. Wang, A. L. Klein, K. C. Patel, J. H. Sherman, M. Keidar, *Materials Adv.* **2020**, *1*(6), 1494.
- [8] K. R. Liedtke, S. Diedrich, O. Pati, E. Freund, R. Flieger, C. D. Heidecke, L. I. Partecke, S. Bekeschus, *Anticancer Res* **2018**, *38*(10), 5655.
- [9] H. Zhang, J. Zhang, Z. Liu, D. Xu, L. Guo, D. Liu, M. G. Kong, *Plasma Process Polym.* **2019**, *16*(12), 1900072.
- [10] J. Zhang, D. Liu, H. Zhang, W. Xia, Y. Liu, B. Sun, D. Xu, L. Guo, M. G. Kong, *Plasma Process Polym* **2020**, *17*(7), 1900213.
- [11] G. Pasqual-Melo, T. Nascimento, L. J. Sanches, F. P. Blegniski, J. K. Bianchi, S. K. Sagwal, J. Berner, A. Schmidt, S. Emmert, K. D. Weltmann, T. von Woedtke, R. K. Gandhirajan, A. L. Cecchini, S. Bekeschus, *Cancers* **2020**, *12*(7).
- [12] E. J. Szili, J. S. Oh, H. Fukuhara, R. Bhatia, N. Gaur, C. K. Nguyen, S. H. Hong, S. Ito, K. Ogawa, C. Kawada, T. Shuin, M. Tsuda, M. Furihata, A. Kurabayashi, H. Furuta, M. Ito, K. Inoue, A. Hatta, R. D. Short, *Plasma Sources Sci. Technol.* **2017**, *27*(1), 014001.
- [13] Z. Chen, H. Simonyan, X. Cheng, E. Gjika, L. Lin, J. Canady, J. H. Sherman, C. Young, M. Keidar, *Cancers (Basel)* **2017**, *9*, 61.
- [14] S. B. Karki, T. T. Gupta, E. Yildirim-Ayan, K. M. Eisenmann, H. Ayan, *J Phys D Appl Phys* **2017**, *50*(31), 315401.
- [15] Z. He, K. Liu, E. Manaloto, A. Casey, G. P. Cribaro, H. J. Byrne, F. Tian, C. Barcia, G. E. Conway, P. J. Cullen, J. F. Curtin, *Sci Rep* **2018**, *8*(1), 5298.
- [16] L. Lin, M. Keidar, *Appl Phys Rev* **2021**, *8*(1), 011306.
- [17] H. R. Metelmann, C. Seebauer, V. Miller, A. Fridman, G. Bauer, D. B. Graves, J. Pouvesle, R. Rutkowski, M. Schuster, S. Bekeschus, K. Wende, K. Masur, S. Hasse, T. Gerling, M. Hori, H. Tanaka, E. Choi, K. Weltman, *Clin Plasma Med.* **2018**, *9*, 6.
- [18] C. Jensen, Y. Teng, *Front Mol Biosci* **2020**, *7*, 7.
- [19] J. Rodrigues, M. A. Heinrich, L. M. Teixeira, J. Prakash, *Trends Cancer* **2021**, *7*(3), 249.
- [20] S. Li, Z. Zhang, L. Han, *Trends Cancer* **2020**, *6*(8), 622.
- [21] E. Colombo, M. G. Cattaneo, *Int J Mol Sci* **2021**, *22*(4), 1633.
- [22] J. Farhat, I. Pandey, M. AlWahsh, *Cells* **2021**, *10*(7), 1657.
- [23] L.-B. Weiswald, D. Bellet, V. Dangles-Marie, *Neoplasia* **2015**, *17*(1), 1.
- [24] L. Carroll, B. Tiwari, J. F. Curtin & J. Wanigasekara, *protocols.io.* **2021**, *1*, 1-6. <https://dx.doi.org/10.17504/protocols.io.bszmnf46>
- [25] L. Scally, S. Behan, A. Carvalho, C. Sarangapani, B. Tiwari, R. Malone, H. J. Byrne, J. F. Curtin & P. J. Cullen, *Plasma Process Polym.* **2021**, *18*, e2000250.
- [26] A. Nandi, L. J. Yan, C. K. Jana, N. Das, *Oxid Med Cell Longev* **2019**, *2019*, 9613090.
- [27] R. S. Joshi, S. S. Kanugula, S. Sudhir, M. P. Pereira, S. Jain, M. K. Aghi, *Cancers* **2021**, *13*(6), 1399.
- [28] A. Chhetri, J. V. Rispoli, S. A. Lelièvre, *Front Mol Biosci* **2021**, *8*(22), 628386.
- [29] A. M. A. de Carvalho, S. Behan, L. Scally, C. Sarangapani, R. Malone, P. J. Cullen, B. Tiwari, J. F. Curtin, *bioRxiv* **2021**, *10*, 1.
- [30] E. Gjika, S. Pal-Ghosh, M. E. Kirschner, L. Lin, J. H. Sherman, M. A. Stepp, M. Keidar, *Sci. Rep.* **2020**, *10*(1), 16495.
- [31] S. K. Singh, S. Abbas, A. K. Saxena, S. Tiwari, L. K. Sharma, M. Tiwari, *Biotechniques* **2020**, *69*(5), 333.
- [32] J. E. Piletz, J. Drivon, J. Eisenga, W. Buck, S. Yen, M. McLin, W. Meruvia, C. Amaral, K. Brue, *Cell Med* **2018**, *10*, 2155179018755140.
- [33] K. Białkowska, P. Komorowski, M. Bryszewska, K. Miłowska, *Int J Mol Sci* **2020**, *21*(17), 6225.

## SUPPORTING INFORMATION

Additional supporting information may be found in the online version of the article at the publisher's website.

**How to cite this article:** J. Wanigasekara, C. Barcia, P. J. Cullen, B. Tiwari, J. F. Curtin. Plasma induced reactive oxygen species-dependent cytotoxicity in glioblastoma 3D tumourspheres. *Plasma Processes Polym.* **2022**;19:e2100157. <https://doi.org/10.1002/ppap.202100157>